Proteomic and functional evidence for a P2X$_7$ receptor signalling complex

**Miran Kim, Lin-Hua Jiang,
Heather L.Wilson, R.Alan North[1] and
Annmarie Surprenant**

Institute of Molecular Physiology, University of Sheffield,
Alfred Denny Building, Western Bank, Sheffield S10 2TN, UK

[1]Corresponding author
e-mail: r.a.north@sheffield.ac.uk

P2X receptors are ATP-gated ion channels in the plasma membrane, but activation of the P2X$_7$ receptor also leads to rapid cytoskeletal re-arrangements such as membrane blebbing. We identified 11 proteins in human embryonic kidney cells that interact with the rat P2X$_7$ receptor, by affinity purification followed by mass spectroscopy and immunoblotting [laminin α3, integrin β2, β-actin, α-actinin, supervillin, MAGuK, three heat shock proteins, phosphatidylinositol 4-kinase and receptor protein tyrosine phosphatase-β (RPTPβ)]. Activation of the P2X$_7$ receptor resulted in its dephosphorylation. Whole-cell recordings from cells expressing P2X$_7$ receptors showed that this markedly reduced subsequent ionic currents and it also slowed membrane bleb formation. By mutagenesis, we identified Tyr^{343} in the putative second transmembrane domain as the site of phosphorylation. Thus, we have identified a P2X$_7$ receptor signalling complex, some members of which may initiate cytoskeletal rearrangements following receptor activation. Others, such as RPTPβ, might exert feedback control of the channel itself through its dephosphorylation.
Keywords: ion channel/P2X receptors/receptor protein tyrosine phosphatase-β/signalling complex/tyrosine phosphorylation

Introduction

P2X receptors form a family of ATP-gated ion channels extensively distributed throughout the cells of vertebrates. They are ligand-gated ion channels, each with distinct pharmacological and/or physiological properties. They form as homomers and/or heteromers, and current biochemical evidence suggests that the channel has three or perhaps six subunits (Nicke *et al*., 1998; North and Surprenant, 2000). The P2X$_7$ receptor subunit has several features that set it apart from other members of the family (Surprenant *et al*., 1996). Co-immunoprecipitation experiments indicate that it is the only subunit that does not heteropolymerize with other P2X subunits (Torres *et al*., 1999). It is primarily localized to epithelia and immune cells, particularly antigen-presenting cells (Collo *et al*., 1997; Mutini *et al*., 1999). Receptor activation requires concentrations of ATP that are 10–100 times higher than those required to activate other P2X receptors, but the

agonist affinity and maximum response can also be modulated 5- to 100-fold by alterations in external monovalent and divalent cations (Surprenant *et al*., 1996; Rassendren *et al*., 1997; Michel *et al*., 1999; Gudipaty *et al*., 2001). The ionic currents through P2X$_7$ receptors show considerable plasticity, in the sense that repeated applications of the agonist result in prominent changes in the amplitude and time course of the current elicited by subsequent applications (Surprenant *et al*., 1996; Rassendren *et al*., 1997; Hibell *et al*., 2000).

Activation of native ATP receptors in macrophages and macrophage-like cell lines, in which P2X$_7$ subunits are predominantly expressed, is fundamentally different from that observed for other ion channels because it initiates several cellular consequences further downstream. These include alterations in the cell morphology (Cohn and Parks, 1967), interleukin-1β release (Ferrari *et al*., 1997a; Solle *et al*., 2001), NFκB activation (Ferrari *et al*., 1997b), phospholipase D activation (Humphreys and Dubyak, 1996), cytolysis and/or apoptosis (Di Virgilio, 2000). The morphological changes are readily seen with heterologous expression of P2X$_7$ receptors in HEK293 cells, where large membrane blebs appear within 30–60 s of activating the receptor (Virginio *et al*., 1999). The changes in cell morphology are not seen with other P2X receptors, suggesting that they may result from direct coupling to cytoskeletal proteins rather than from the flow of ionic current. In support of this notion is our recent observation that rat P2X$_7$ receptors heterologously expressed in HEK293 cells as well as native P2X$_7$ receptors in rat peritoneal macrophage appeared as a strongly bound multimeric complex, which seemed unlikely to be comprised solely of P2X$_7$ receptor subunits (Kim *et al*., 2001).

Here we have identified 11 proteins that interact with the rat P2X$_7$ receptor. These are the extracellular matrix protein laminin α3, the membrane-spanning proteins integrin β2 and receptor protein tyrosine phosphatase β (RPTPβ) and eight intracellular proteins [α-actinin 4, β-actin, supervillin, three heat shock proteins (Hsp90, Hsc71 and Hsp70), phosphatidylinositol 4-kinase 230 (PI4K) and membrane-associated guanylate kinase P55 (MAGuK)]. We further show that the P2X$_7$ receptor becomes dephosphorylated at Tyr^{343} upon activation, and that this strongly inhibits the membrane current and retards membrane blebbing. These results suggest that RPTPβ and other associated proteins are key molecular elements in downstream signalling from P2X$_7$ receptors to the cytoskeleton, and that one aspect of that signalling is feedback control of the channel function.

Results

Identification of interacting proteins
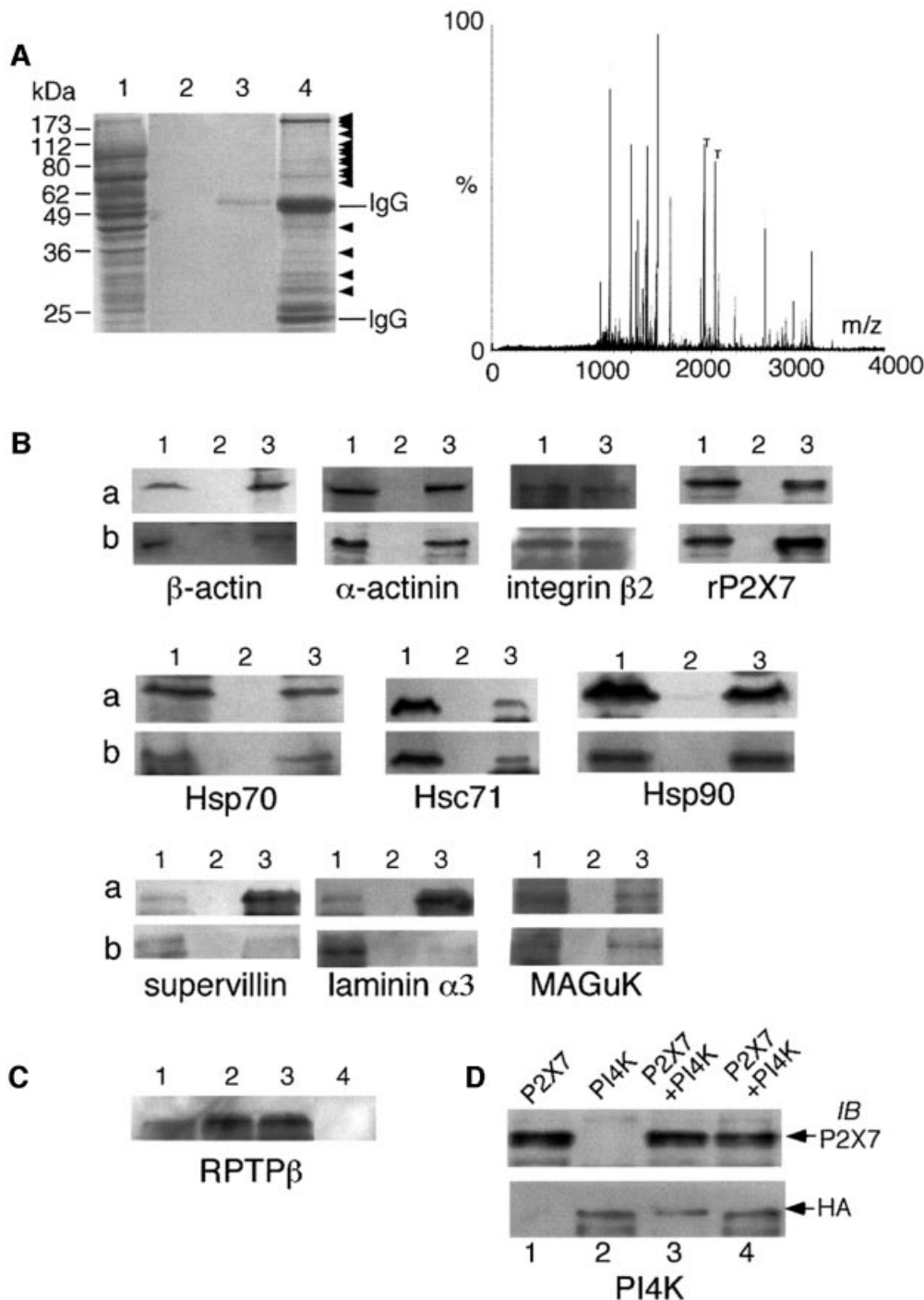The receptor complex was isolated by immunoprecipitation with ecto-P2X$_7$ antibody (Ab) using purified

Fig. 1. Proteomic characterization of P2X$_7$ receptor protein complex. (**A**) Protein staining of SDS–PAGE membrane extracts from HEK cells stably expressing P2X$_7$ receptors. Lane 1 is total membrane extract; lanes 2 and 3 are negative controls showing membrane extracts bound to γ-bind G-Sepharose and after immunoprecipitation with an anti-P2X$_2$ Ab, respectively. Lane 4 shows protein staining after immunoprecipiteads show position of bands excised for mass spectroscopy. IgG bands were identified by N-terminal amino acid sequencing. Right-hand panel shows MALDI-TOF spectrum of the 70 kDa protein band after digestion with trypsin; 'T' labels peptide from trypsin autolysis. The remaining peaks match peptides from Hsp70. (**B**) Blotting with antibodies to β-actin, α-actinin, integrin β2, P2X$_7$ receptor, Hsp70, Hsc71, Hsp90, supervillin, laminin α3 and MAGuK-p55 (as indicated) from membrane fractions (a) from HEK293 cells stably expressing P2X$_7$ receptors or (b) from HEK293 cells transiently expressing P2X$_7$-EE receptor. In each case, lane 1 is solubilized membrane fraction, lane 2 is negative control with mouse IgG, and lane 3 is from IP with ecto-P2X$_7$ or EE Ab. (**C**) Blots with anti-RPTPβ Ab. Lane 1 is membrane fraction, lane 2 is IP with ecto-P2X$_7$ Ab from P2X$_7$-expressing cells (stable transfection), lane 3 is IP with anti-EE Ab from P2X$_7$-EE-expressing cells (transient transfection), and lane 4 is negative control with mouse IgG. (**D**) Co-expression of P2X$_7$-EE and PI4K-HA cDNA (lanes 3 and 4). Lane 1, P2X$_7$-EE cDNA only; lane 2, PI4K-HA cDNA only. Lanes 1 and 3, IP with anti-EE Ab; lanes 2 and 4, IP with anti-HA Ab; membranes blotted with anti-P2X$_7$ or anti-HA as indicated.

membrane fractions of HEK293 cells stably expressing the rat P2X$_7$ receptor (Kim *et al.*, 2001). When the receptor complex was separated by SDS–PAGE and stained with Coomassie Blue, numerous bands ranging in size from <25 to 250 kDa were apparent (Figure 1A, lane 4). These were not present in membrane extracts bound to the γ-bind

Table I. Proteins identified in the P2X$_7$ receptor complex by MALDI-TOF MS and confirmed by western blotting

Protein name	Abbreviation	Molecular weight (kDa)	SwissProt/Trembl	Peptides[a]
Extracellular				
laminin α3 chain		187	Q16787	7 (2, 3)[b]
Transmembrane				
integrin β2		85	P05107	9
protein tyrosine phosphatase β	RPTPβ	222	P23467	8 (2, 2)[b]
Intracellular				
β-actin		42	P02570	9
α-actinin 4		105	O43707	6
heat shock cognate 71 kDa protein	Hsc71	71	P11142	15
heat shock 70 kDa protein 1	Hsp70	70	P08107	16
heat shock protein HSP90-β	Hsp90	83	P08238	9
phosphatidylinositol 4-kinase 230	PI4K	231	Q9UPG2	8 (3, 4)[b]
MAGUK P55 subfamily member 3	MAGuK	66	Q13368	6
supervillin		201	O60611	9 (3, 1)[b]

[a]The number of peptides matched following trypsin digestion.
[b]Numbers in parentheses indicate endo-Arg-C and endo-Asp-N digestions.

G-Sepharose used in the immunoprecipitations nor from those immunoprecipitated with anti-P2X$_2$ Ab (Figure 1A, lanes 2 and 3). Bands indicated by arrowheads in Figure 1A were excised, subjected to peptic digest with trypsin, endoprotease Arg-C or Asp-N, and identified by matrix-assisted laser desorption/ionization time-of-flight (MALDI-TOF) mass spectroscopy (MS). One example of results obtained for the protein identified as heat shock protein Hsp70 is shown in Figure 1A. Eleven proteins were unambiguously identified (Table I). These comprised of the extracellular matrix protein laminin α3, three cyto-skeletal proteins (α-actinin 4, β-actin, supervillin) and an integrin subunit (β2), one scaffolding protein (MAGuK), three chaperones (Hsp90, Hsp70, Hsc71) and two signall-ing proteins (RPTPβ and PI4K). N-terminal amino acid sequencing was also used to identify the IgG bands indicated in Figure 1A.

We next used immunoblotting to provide direct bio-chemical evidence for physical association of these proteins within the P2X$_7$ receptor complex. We pulled down the receptor complex from HEK293 cells stably expressing the P2X$_7$ receptor using ecto-P2X$_7$ Ab or from HEK293 cells transiently transfected with a C-terminal epitope-tagged P2X$_7$ receptor cDNA (P2X$_7$-EE) using anti-EE Ab. We then blotted antibodies to the 11 identified proteins (Figure 1B–D). All eleven proteins indi-vidually co-immunoprecipitated with the P2X$_7$ receptor (Figure 1B–D; Table I).

Tyrosine phosphorylation of the P2X$_7$ receptor

The identification of RPTPβ as an associated protein in the P2X$_7$ receptor complex allowed the possibility that the receptor itself could be phosphorylated on tyrosine(s). Therefore, we incubated P2X$_7$-expressing HEK cells for 5–30 min in the presence or absence of the pervanadate analogue bisperoxo-(1,10-phenanthrolone)-oxovanadate (bpV), a cell-permeable protein tyrosine phosphatase inhibitor (Posner *et al.*, 1994). We immunoprecipitated the receptor complex using the ecto-P2X$_7$ Ab for stable cell lines or the anti-EE Ab for transiently transfected cells (mouse IgG was the negative control). The

immunoprecipitated proteins were separated by SDS–PAGE, transferred to PVDF membranes and detected using the anti-phosphotyrosine antibody PY20. A phos-photyrosine protein running at the expected size of the P2X$_7$ receptor subunit was detected; this was directly confirmed as the P2X$_7$ receptor by stripping the membrane and re-probing with a C-terminal anti-P2X$_7$ receptor Ab (Figure 2A). Although equal amounts of P2X$_7$ receptor subunit protein were immunoprecipitated from untreated and bpV-treated cells, only the P2X$_7$ receptor from bpV-treated cells showed detectable levels of tyrosine phos-phorylation (Figure 2A, lanes 3 and 6). We found that 5 min incubation with bpV (100 μM) was sufficient to induce tyrosine phosphorylation of the receptor (data not shown; $n = 3$). We also examined the concentration dependence of this tyrosine phosphatase inhibitor. Incubation of cells for 10 min with 10, 100 or 500 μM bpV (but not 1 or 3 μM) resulted in detectable tyrosine phosphorylation of the P2X$_7$ receptor ($n = 3$). When P2X$_7$ receptors were activated by exposing cells to the ATP analogue 2′,3′-O-(benzoyl-4-benzoyl)ATP (BzATP, 100 μM) for 10 min prior to and during the 10 min incubation with bpV, significantly lower levels of tyrosine phosphorylation of the receptor were detected (Figure 2A, lane 4). However, no decrease in levels of tyrosine phosphorylation of the P2X$_7$ receptor occurred if cells were first exposed to bpV for 10 min after which BzATP (in the continued presence of bpV) was added for 10 min (Figure 2B, lanes 2 and 3). ATP (1 mM) produced similar results to those obtained with BzATP ($n = 3$). These results suggest a tonic activity of a tyrosine phosphatase at the P2X$_7$ receptor, which is significantly increased upon activation of the receptor by agonists.

We obtained similar results with other protein tyrosine phosphatase inhibitors; these were the pervanadate analogue monoperoxo-(picolinato)-oxovanadate (mpV), and the structurally unrelated inhibitor 3,4-dephostatin (Figure 2B). With these phosphatase inhibitors we observed that activation of the P2X$_7$ receptor prior to but not during or after phosphatase inhibition also resulted in decreased levels of tyrosine phosphorylation of the receptor (Figure 2B, lanes 5 and 6 for BzATP simultaneous
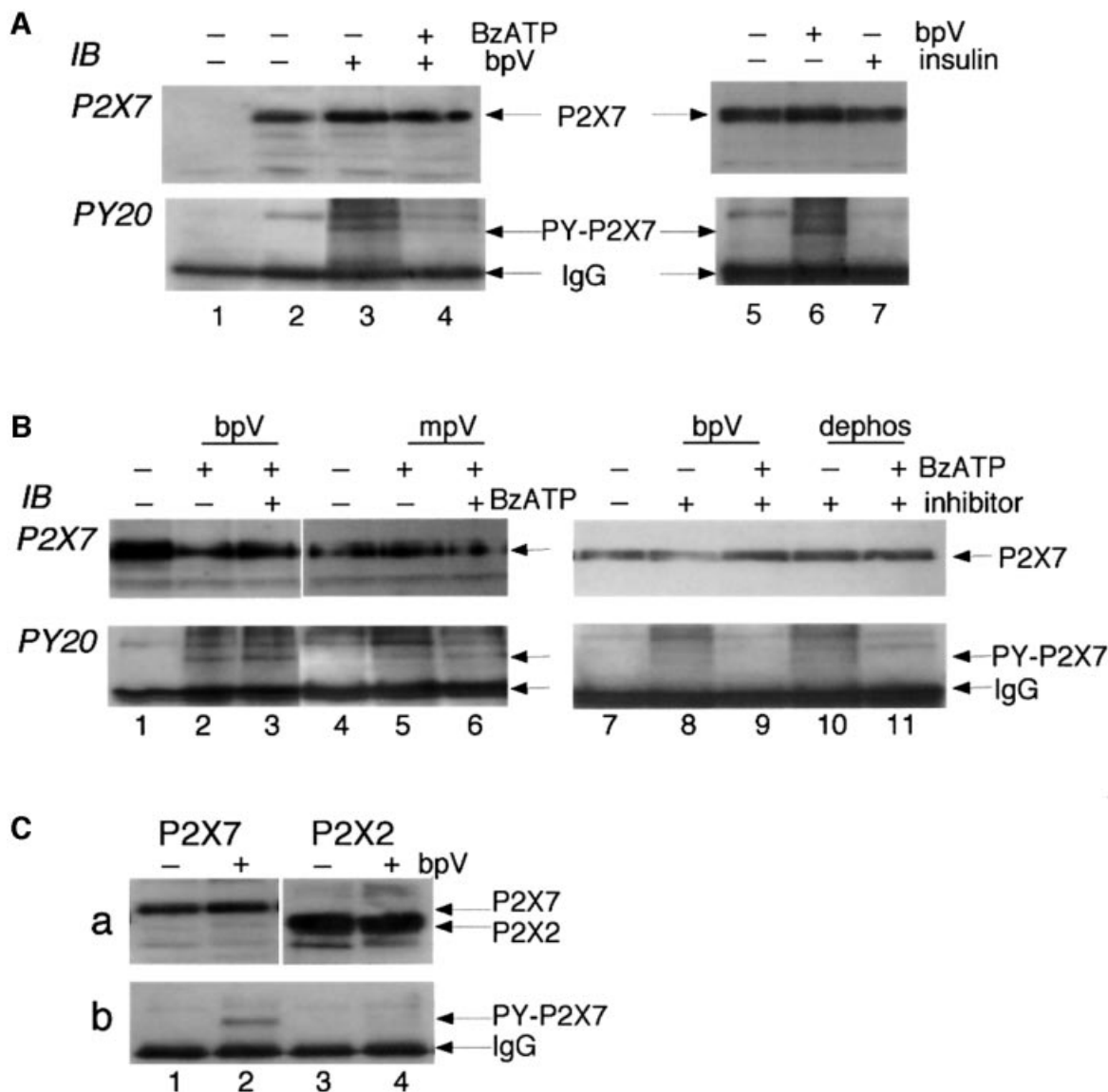
Fig. 2. Tyrosine phosphorylation of P2X$_7$ receptor. (**A**) Membrane extracts from untransfected (lane 1, negative control) or P2X$_7$ receptor-expressing HEK293 cells were immunoprecipitated with ecto-P2X$_7$ Ab, and phosphotyrosine incorporation into the P2X$_7$ protein was detected by probing with anti-phosphotyrosine Ab PY20. The blot was then stripped and re-probed with C-terminal anti-P2X$_7$ Ab to confirm that the phosphotyrosine bands (lanes 3, 4 and 6) were the P2X$_7$ receptor. No tyrosine phosphorylation was detected in control P2X$_7$-expressing cells (lanes 2 and 5) but after 10 min incubation with the tyrosine phosphatase inhibitor bpV (100 μM) phosphotyrosine was clearly detected (lanes 3 and 6). The level was much reduced if the P2X$_7$ receptor was activated for 10 min with BzATP (100 μM) prior to incubation with bpV (lane 4). (**B**) Similar experiments using phosphatase inhibitors mpV (100 μM, lanes 5 and 6) or 3,4-dephostatin (100 μM, lanes 10 and 11) also show tyrosine phosphorylation of P2X$_7$ subunit in the presence of the phosphatase inhibitors (lanes 5 and 10), which is reduced when BzATP is added prior to application of phosphatase inhibitor (lane 11), but not when BzATP is added after the phosphatase inhibitor (lanes 3 and 6). (**C**) Tyrosine phosphorylation occurs on P2X$_7$ receptor but not P2X$_2$ receptor. Similar experiment to others performed on HEK cells transiently transfected with P2X$_7$-EE (lanes 1 and 2) or P2X$_2$-EE (lanes 3 and 4) receptors. Immunoprecipitation was with anti-EE Ab in the absence or presence of bpV as indicated. Anti-PY20 blotting detected phosphotyrosine-P2X$_7$ after bpV treatment (b, lane 2) but no tyrosine phosphorylation of P2X$_2$ receptor (b, lanes 3 and 4). Stripping and re-probing with C-terminal anti-P2X$_7$ (a, lanes 1 and 2) or anti-P2X$_2$ (a, lanes 3 and 4) confirms tyrosine phosphorylation of P2X$_7$ but not P2X$_2$ receptor even though there is greater expression of P2X$_2$ protein.

with mpV, lanes 10 and 11 for BzATP prior to 3,4-dephostatin). Because bpV can also activate insulin receptor kinase (Posner *et al.*, 1994) and because some HEK293 cells have been reported to express insulin receptors (Kellerer *et al.*, 1997), we asked whether exposure to insulin (100 nM for 30 min) might lead to P2X$_7$ receptor tyrosine phosphorylation. It did not (Figure 2A, lane 7).

Tyrosine phosphorylation was not generalized to other members of the P2X receptor family. We transfected maximal concentrations of cDNA encoding either P2X$_7$-EE or P2X$_2$-EE receptors into HEK293 cells, immmuno-precipitated with anti-EE Ab, and separated the proteins on SDS–PAGE. The amount of P2X$_2$ receptor protein was always 3- to 5-fold greater than that of P2X$_7$ receptor protein (Figure 2C; *n* = 4). However, no tyrosine
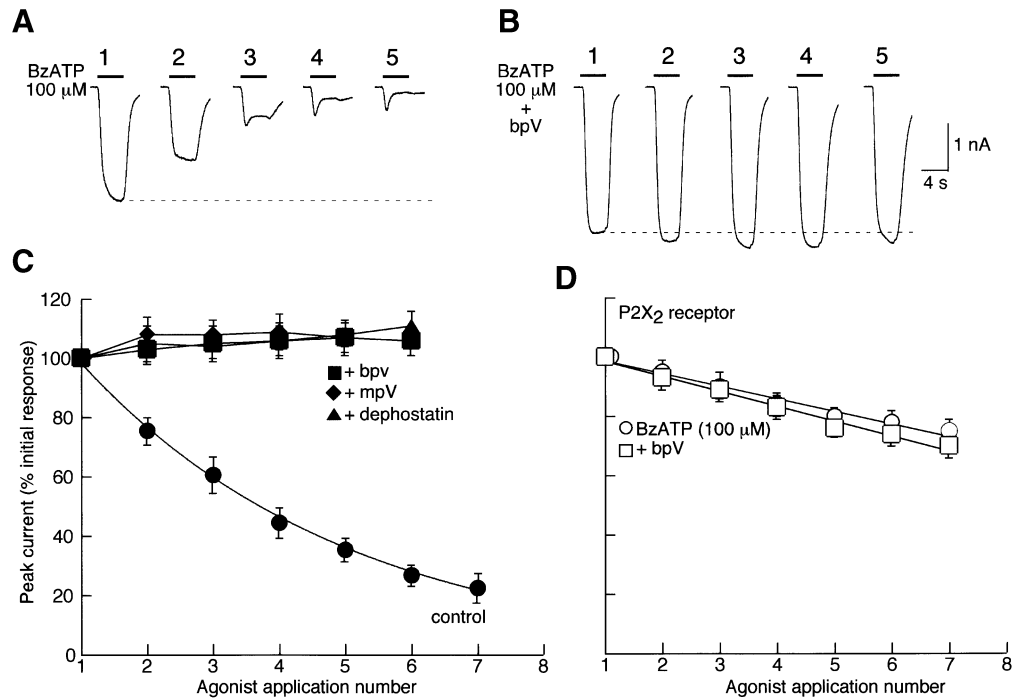
Fig. 3. Functional evidence for use-dependent tyrosine dephosphorylation of P2X$_7$ receptor. (**A**) Currents in response to successive applications of 100 µM BzATP (4 s duration, indicated by bars) at 2 min intervals; note the marked change in kinetics of the current. (**B**) Currents recorded from another cell in response to successive applications of 100 µM BzATP in the presence of the tyrosine phosphatase inhibitor bpV (100 µM). (**C**) Summary of results from all experiments as illustrated in (A) and (B) (*n* = 43 for each point in control and 7–13 for each point in any of the phosphatase inhibitors). (**D**) Similar experiments performed on P2X$_2$-expressing HEK cells. Minimal run-down occurs with successive stimuli and is unaltered by bpV (100 µM; *n* = 6–12 for each point). All results were obtained from HEK cells stably expressing P2X$_7$ (A–C) or P2X$_2$ (D) receptors.

phosphorylation of the P2X$_2$ receptor could be detected in the control or bpV-treated cells (Figure 2C).

Functional modulation of P2X$_7$ receptor by tyrosine phosphorylation

To test for a possible functional consequence of P2X$_7$ receptor phoshorylation, we recorded whole-cell currents from HEK293 cells expressing P2X$_7$ receptors during repeated applications of BzATP or ATP. Brief (4 s duration, 2 min intervals) applications of agonist at high concentrations (100–300 µM BzATP; 1–3 mM ATP) evoked inward currents that showed a marked run-down in amplitude; during the run-down the current became distinctly biphasic, consisting of an initial transient and subsequent smaller sustained current (Figure 3A). The run-down depended on the total duration of agonist application and not on duration of whole-cell recording (i.e. dialysis) or intracellular pipette solution. That is, the peak current declined approximately exponentially (time constant 4.6 ± 0.2 min, *n* = 9), and at steady-state it had run-down to 21 ± 2% of initial peak current (Figure 3A and C). When BzATP was initially applied for 30 s, the peak amplitude of the current evoked by the test (4 s duration) application 2 min later was 18 ± 4% (*n* = 4). Moreover, no obvious differences in the run-down were apparent when the patch pipette contained NaCl, KCl, Na-aspartate, K-aspartate, CsCl, or when intracellular calcium was strongly or weakly buffered using 4 mM BAPTA/ 10 mM EGTA or 0.1 mM EGTA/0.5 mM CaCl$_2$, respectively. There were no significant differences in the time course of development or steady-state level of

run-down from cells, in which the agonist was first applied 0.5 or 12 min after establishing whole-cell conditions (*n* = 4), nor were there significant differences if an ATP-regenerating cocktail (Rosenmund and Westbrook, 1993) was included in the patch pipette (*n* = 8). Finally, the run-down of the currents did not depend on the direction of current flow; the kinetics of the responses and the time-course of the run-down were the same at –60 mV (inward current) and 30 mV (outward current, *n* = 4). When using sub-maximal concentrations (i.e. 30 µM BzATP or 500 µM ATP), inward currents increased in amplitude and deactivated more slowly with repeated applications ('run-up' data not shown). This current run-up has been described in detail in previous studies (Surprenant *et al.*, 1996; Hibell *et al.*, 2000) and has not been further examined in the present study.

The run-down was not observed when any one of the three phosphatase inhibitors was present in the superfusion solution (Figure 3B and C). Repeated applications of agonist elicited currents with similar kinetics, and their peak amplitude showed a small (5–20%) increase with successive applications (Figure 3B and C). Additionally, the current elicited by the first application of BzATP (100 µM) was up to 3-fold greater in cells treated with phosphatase inhibitors than in control cells (peak amplitudes were: control 1720 ± 145 pA, bpV-treated 3000 ± 239 pA, *n* = 47 for each; Figure 3B). The agonist half-maximal concentrations (EC$_{50}$ values) were not significantly different (*n* = 4) in the presence of tyrosine phosphatase inhibitors. The effect of the phosphatase inhibitors was fully reversible; within 6–20 min of
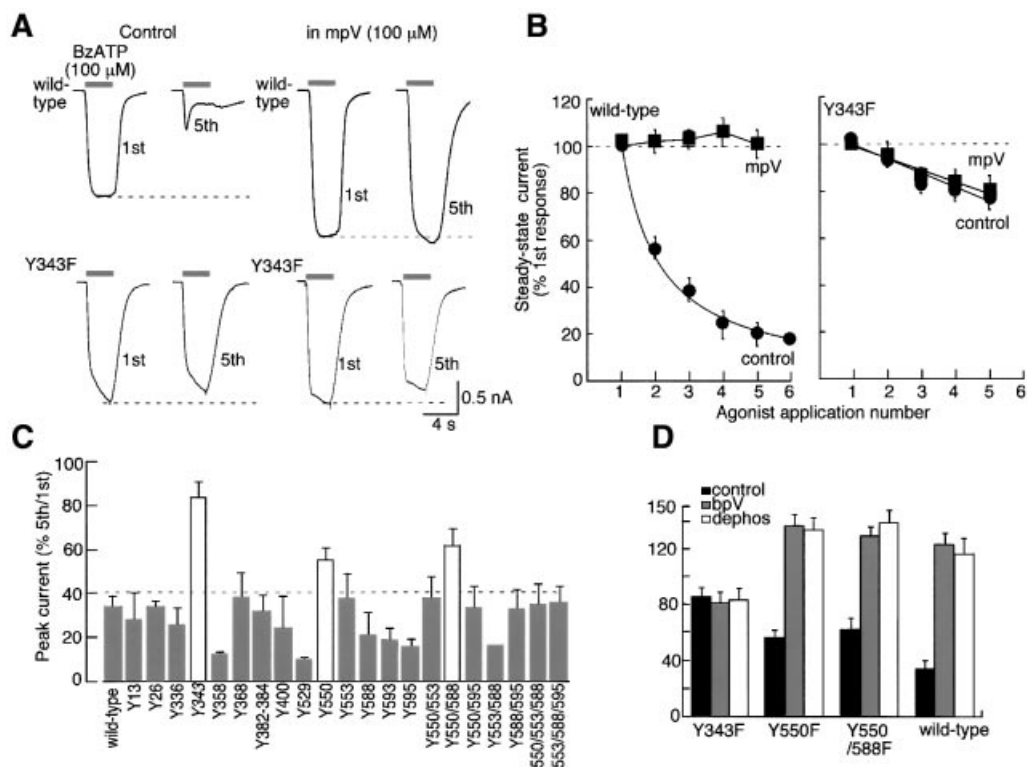
Fig. 4. Mutation of Tyr[343] prevents run-down of current and effect of phosphatase inhibitors. (**A**) Currents recorded from wild type (upper traces) and Y343F (lower traces) in response to BzATP (100 μM). Left traces are from cells in normal solution and right traces are cells in mpV (100 μM). (**B**) Current amplitude at end of 4 s duration application of BzATP as a function of agonist application number for all experiments with HEK cells transiently transfected with wild type (left; $n = 12–24$) and Y343F (right; $n = 6$ each) P2X$_7$ receptor. (**C**) Summary of tyrosine mutagenesis of P2X$_7$ receptor. Histogram shows BzATP-evoked current as a percentage of amplitude of 5th/1st application; only Y343F and Y550F or Y550/588F (white bars) show significantly less run-down than wild type. (**D**) Phosphatase inhibitors (bpV and dephostatin) have no effect on Y343F but affect Y550F and Y550/588F to the same extent as at the wild-type receptor; data are plotted as in (C); $n = 3$ for each mutant, 13 for wild type.

washout the current evoked by BzATP (100 μM) had run-down by approximately the same amount ($32 \pm 12\%$ of initial current amplitude, $n = 9$). The EC$_{50}$ for bpV was 5 ± 0.4 μM with a Hill slope of 3.3 ± 0.7 ($n = 6$; see Materials and methods).

When P2X$_2$ receptors are expressed in HEK293 cells, repeated applications of high agonist concentrations also produce a run-down of the evoked current, although this is of much lower magnitude than at the P2X$_7$ receptor and occurs without any change in the kinetics of the response. Application of bpV (100 μM; up to 16 min) did not alter the amplitude or kinetics of run-down of the P2X$_2$ currents (Figure 3D; $n = 6$). The lack of effect of phosphatase inhibitors on ATP-evoked currents at P2X$_2$ receptors is in keeping with the lack of tyrosine phosphorylation of this protein observed with immunoblots and suggests that this modulation is likely to be P2X$_7$ receptor specific.

Our experiments indicate that the resting P2X$_7$ receptor is phosphorylated on tyrosine but we did not identify any associated tyrosine kinase by affinity purification. Several other channels can be tyrosine phosphorylated by Src family kinases [e.g. Kv1.3 potassium channels (Holmes *et al.*, 1996), maxi-K channels (Ling *et al.*, 2000), γ-aminobutyric acid receptors (Moss *et al.*, 1995), NMDA receptors (Yu *et al.*, 1997; Zheng *et al.*, 1998; Vissel *et al.*, 2001; Yang and Leonard, 2001)]. However, inclusion of c-Src in the patch pipette ($n = 7$) or co-expression of v-Src and P2X$_7$ receptor cDNAs ($n = 7$) did

not significantly alter the time course, kinetics or extent of current run-down produced by 100 μM BzATP. The peak amplitude of the initial responses was also not significantly different from control responses. Moreover, c-Src did not co-immunoprecipitate with P2X$_7$ receptors in immunoblot experiments (data not shown).

Identification of Tyr[343] as a substrate for tyrosine phosphorylation

There are two tyrosines in the short intracellular N-terminus of the rat P2X$_7$ receptors and 12 in the longer intracellular C-termini of the protein; only one of these (Tyr[13]) is conserved among all P2X receptors. We first mutated each of these 14 tyrosines to phenylalanine and compared the amplitudes, kinetics and run-down of the currents, as well as the effects of bpV (100 μM), using our standard protocol (4 s duration of 100 μM BzATP at 2 min intervals). All mutants were approximately equally expressed in the plasma membrane, as assessed by immunohistochemistry using ecto-P2X$_7$ Ab and confocal microscopy (Kim *et al.*, 2001). Only Y550F differed significantly from the wild type in showing minimal change in current kinetics with repeated stimuli and less run-down (Figure 4C). However, the actions of bpV and 3,4-dephostatin were the same as for the wild-type receptor (Figure 4D), and the P2X$_7$[Y550F] receptor protein was equally tyrosine phosphorylated in the presence of bpV (Figure 5B). Several of these tyrosines
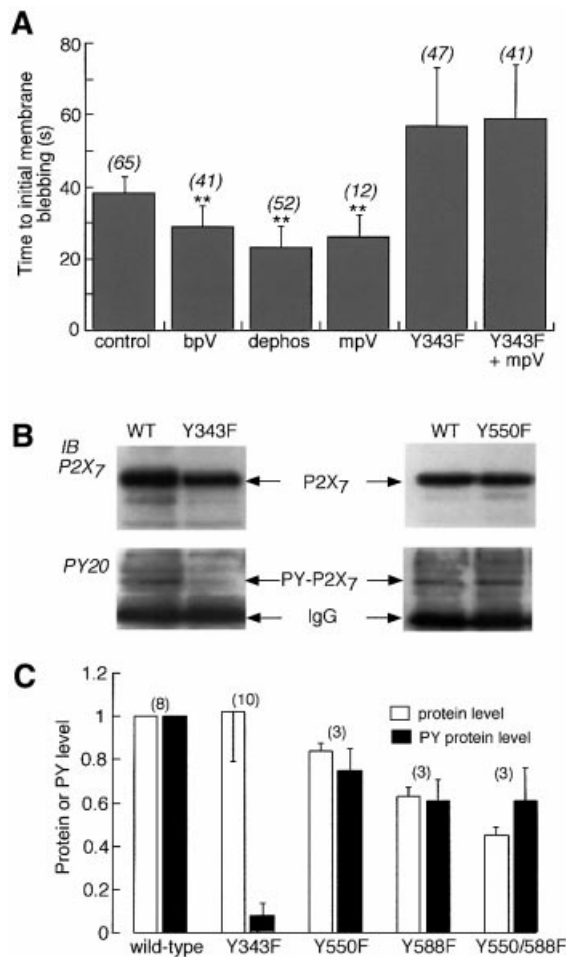
Fig. 5. P2X$_7$ receptor signalling to the cytoskeleton is modulated by phosphorylation of Tyr^{343}. (**A**) Time to initial membrane blebbing in response to application of 100 µM BzATP. Phosphatase inhibitors (100 µM) significantly decreased time to initial blebbing ($p < 0.0001$) in wild type but not in Y343F mutant. Numbers in parentheses are number of cells. (**B**) Tyrosine phosphorylation of P2X$_7$ receptor is markedly reduced in Y343F mutant. Immunoblots for wild type and Y550F or wild type and Y343F are shown. In each case anti-EE Ab was used for immunoprecipitation from cells transiently transfected with P2X$_7$-EE receptor. Tyrosine phosphorylation was then detected with anti-PY-20 Ab, after which the membrane was stripped and re-probed with anti-P2X$_7$ Ab. In all cases bpV (100 µM) was present for 10 min prior to membrane extraction. Tyrosine phosphorylation of wild type and Y550F was observed, but not Y343F. (**C**) Densitometric analysis of wild-type and mutant P2X$_7$ receptors. Each protein band (P2X$_7$, open bars; tyrosine phosphorylated P2X$_7$, closed bars) was scanned using GeneGenius and raw data were normalized to that of wild type.

were also mutated in pairs and triplets but no significant differences from the wild type were observed of those that expressed well (Figure 4C).

There are also two tyrosines in the second hydrophobic domain, which is presumed to be membrane spanning (Figure 6). The Y336F (and Y336C) mutants were similar in their properties to wild-type receptors. However, P2X$_7$ receptors with point mutations Y343F or Y343C showed no significant run-down of the current with repeated agonist applications, showed no change in the kinetics of the current and showed no effect of bpV, mpV or 3,4-dephostatin (Figure 4). In these mutated receptors, the initial response to BzATP was approximately the same as

the wild-type receptor. Immunoblotting detected little or no tyrosine phosphorylation of P2X$_7$[Y343F] receptor (Figure 5B and C).

We asked whether phosphorylation at Tyr^{343} might also be involved in the other signals from the P2X$_7$ receptor, independent of the flow of ionic current. We measured the time to appearance of the first membrane bleb in response to sustained application of 100 µM BzATP (Virginio et al., 1999) in the wild type and in all the tyrosine mutated receptors; only Y550F and Y343F showed altered kinetics of initial blebbing (Figure 5A). For the wild-type receptor, tyrosine phosphatase inhibitors all reduced the time to the appearance of membrane blebbing. In the Y343F receptor, this time was increased and it was not affected by mpV (Figure 5A).

Discussion

P2X$_7$ receptor signalling complex
Activation of the P2X$_7$ receptor not only opens a cation-permeable ion channel, it also results in the activation of several disparate downstream signalling pathways and re-arrangement of the cytoskeleton (see Introduction). We have now identified 11 proteins that form part of a P2X$_7$ receptor signalling complex when it is expressed in HEK293 cells. In broad terms these comprise structural proteins (extracellular, laminin α3; transmembrane, integrin β2 subunit; cytoskeletal, β-actin, α-actinin 4, super-villin, Hsp90, Hsp70, Hsc71, MAGuK) and signalling proteins (PI4K and RPTPβ). These are listed in Table I and summarized schematically in Figure 6A. Whereas some of these proteins have also been found in other ion channel complexes (e.g. the NMDA receptor complex; Husi et al., 2000; Sheng and Pak, 2000), several have not previously been described to associate with membrane ion channels (e.g. PI4K, supervillin, integrin β2).

Laminin α3 may associate directly with the ectodomain of the P2X$_7$ receptor but it is also possible that it is found in the complex because of its binding to integrin β2. Laminins containing the α3 subunit are known to bind to integrins α3β1, α6β4 and α6β1 (Colognato and Yurchenco, 2000), although there is only limited evidence for the involvement of β2 integrins (Bohnsack et al., 1990). Integrin β2 is predominantly expressed by leukocytes, and an 11-amino acid sequence in the C-terminus interacts directly with α-actinin (Sampath et al., 1998). α-actinin and supervillin both interact directly with β-actin. α-actinin head-to-tail dimers cross-link the fibres of β-actin into a regular array and are also involved in anchoring membrane proteins to the cyto-skeleton (see below). Supervillin is also an F-actin binding protein in the villin/gelsolin family (Pestonjamasp et al., 1997).

MAGuK is encoded by the gene discs large homolog 3 (dlg3); it is a scaffolding protein containing several binding domains (PDZ, SH3, GK; Dimitratos et al., 1999). Some MAGuK family members have been implicated in the anchoring of other ion channels to the cytoskeleton. Thus, the C-terminal sequences of several potassium channels and ligand-gated channels bind directly to PDZ and SH3 domains of MAGuK (Sheng and Pak, 2000). The P2X$_7$ receptor does not have such a C-terminal sequence but it does have proline-rich regions
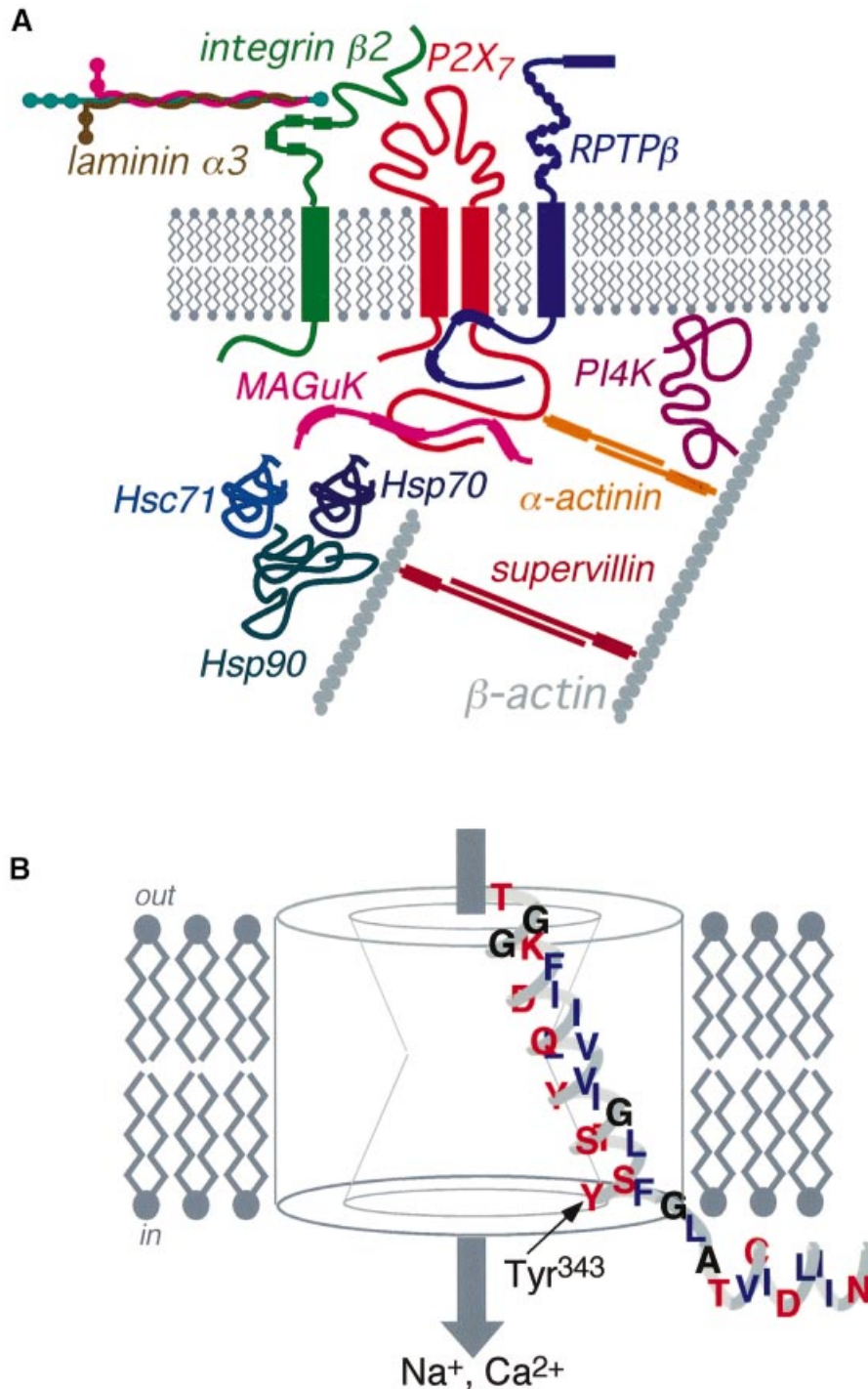
Fig. 6. Schematic summary of P2X$_7$ receptor signalling complex. (**A**) Depiction of P2X$_7$ receptor and interacting proteins identified. Laminin is a heterotrimeric extracellular matrix molecule; the α3 subunit is found in laminin-5, laminin-6 and laminin-7 (Colognato and Yurchenko, 2000). RPTPβ indicates the 230 kDa form of RPTPβ; the extracellular part of the molecule has an N-terminal carbonic anhydrase domain and 16 fibronectin type 3 domains, and the intracellular part has one or two tyrosine phosphatase catalytic domains (Fischer *et al.*, 1991). Integrin β2 is a subunit of hetero-dimeric integrin receptors Mac1 (cd11b, αMβ2) and LFA (cd11a, αLβ2); its cytoplasmic C-terminus can bind to α-actinin (Sampath *et al.*, 1998). α-actinin indicates α-actinin 4, an actin-bundling protein. This forms a reciprocal homodimer, with the two N-terminal actin binding domains at either end. It also has two calponin homology domains, four spectrin repeats and two EF hands. Supervillin is also an F-actin bundling protein that associates with the plasma membrane; it has multiple actin-binding domains and a villin/gelsolin homology domain (Wulfkuhle *et al.*, 1999). PI4K is phosphatidylinositol 4-kinase 230; its domains include an N-terminus SH3 domain, two proline-rich regions, two leucine-zippers, a pleckstrin homology domain and the C-terminal catalytic domain (Gehrmann and Heilmeyer, 1998). MAGuK is membrane-associated guanylate kinase P55 subfamily 3; it contains PDZ, SH3 and GUK domains (Dimitratos *et al.*, 1999). Hsp90 is heat shock protein 90-β. Hsp70 is heat shock protein 70 kDa 1. Hsc71 is heat shock cognate 71 kDa protein. See Table I and text for further information. (**B**) Depiction of the second hydrophobic domain of the P2X$_7$ receptor (Thr^{325}–Asn^{356}) as a membrane-spanning α-helix. Residues are coloured as follows: blue, hydrophobicity index >2.5 (probably lipid facing); red, polar or charged (protein- or pore-facing); black, non-polar. Some residues are partially hidden; the complete sequence is **TGGKF**DIIQLVVYIGSTLSYF**G**LATVCI**D**LIIN. The first two-thirds of the helix might span the membrane and expose Tyr^{343} (arrow) at the inner juxtamembrane region. Residues conserved among all P2X subunits are shown in bold (Gly^{328}, G^{329}, Lys^{330}, Phe^{331}, Gly^{345} and Asp^{353}).

that might engage the SH3 domain of MAGuK; one of these (Pro[450]-Pro-Ile-Pro) forms a canonical SH3-binding sequence. A further possibility is that α-actinin 4 directly anchors the P2X$_7$ receptor to β-actin. The glutamate receptor NR1 subunit has been shown to bind to α-actinin 2 by a region 860–866 (KNLQDRK) in its C-terminal domain (Krupp *et al*., 1999); a homologous sequence appears in the P2X$_7$ receptor at residues 419–425 (KSLQDVK). The heat shock proteins Hsp90 and Hsp70 are well known to associate with each other, although this requires further proteins including Hop (Caplan, 1999). They could be involved in the P2X$_7$ receptor complex through their association with actin (Koyasu *et al*., 1986).

PI4K catalyses the addition of phosphate to the 4-position of phosphatidylinositol (PI), which is the first committed step in the formation of further bis-, tris- and tetra-phosphorylated forms. Clearly, the formation of PI 4,5-bisphosphate (PIP$_2$) could provide the P2X$_7$ receptor with the ability to signal downstream through inositol trisphosphate and diacylglycerol. PIP$_2$ generation would also provide a mechanism for the activation of phospholipase D resulting from P2X$_7$ receptor activation (Humphreys and Dubyak, 1996). PI4Ks have a well conserved domain structure (Gehrmann and Heilmeyer, 1998) and this suggests at least two ways in which PI4K could associate directly with the P2X$_7$ receptor. The proline-rich region of the P2X$_7$ receptor could bind to the N-terminal SH3 domain of PI4K, or it could interact through leucine-zippers. PI4K has two leucine-zipper domains, with five and four leucines. We note that the C-terminus of the P2X$_7$ receptor has a region that is predicted to be α-helical (beginning at Leu[512]) and that might provide one partner to a leucine-zipper interaction.

The last of the 11 proteins identified in the present work was RPTPβ. This prompted us to examine the possibility that the P2X$_7$ receptor itself might be a substrate for tyrosine phosphorylation and dephosphorylation and that this would be reflected in altered channel function.

Receptor dephosphorylation and regulation of channel function

Our biochemical studies show that tyrosine phosphorylation of the P2X$_7$ receptor protein itself can be observed in cells exposed to tyrosine phosphatase inhibitors for as little as 5–10 min, but that activation of P2X$_7$ receptors prior to addition of phosphatase inhibitors yielded a much reduced level of tyrosine phosphorylation of the receptor. This implies that the liganded receptors cannot be readily phosphorylated. Extracellular ATP has previously been shown to dephosphorylate proteins on tyrosine in the mouse leukaemia cell line L1210, and vanadate prevented downstream signalling to apoptosis (Bronte *et al*., 1996). One of the proteins dephosphorylated in these experiments was a 76 kDa protein perhaps corresponding to a P2X$_7$ receptor subunit.

Our functional studies indicate that under the present experimental conditions a phosphatase, perhaps RPTPβ, is tonically active at low levels to dephosphorylate the unliganded P2X$_7$ receptor and that this activity is much increased upon receptor activation. This dephosphorylation results in the strong run-down of the current and a reduced ability to couple to cytoskeletal changes (e.g. membrane blebbing). Essentially similar, if less marked,

effects on membrane currents of tyrosine phosphatase inhibitors have recently been reported for the NMDA receptor heterologously expressed in HEK cells; run-down of currents at high glutamate concentrations was also found to be due to a use-dependent tyrosine dephosphorylation of the NMDA receptor, which was independent of ion flux (Vissel *et al*., 2001). The voltage-gated sodium channel has been shown recently to associate with RPTPβ; inhibition of the enzyme causes a 6 mV hyperpolarizing shift in the voltage dependence of inactivation and thus inhibits the peak current (Ratcliffe *et al*., 2000). In that study, RPTPβ was found to interact with both extracellular and intracellular regions of the sodium channel but its target tyrosine was not identified.

We made amino acid substitutions of phenylalanine for tyrosine at each of sixteen positions (Figure 4). In only two cases did we observe an alteration in the phenotype based on agonist-evoked currents and time to membrane blebbing; these were Y550F and Y343F. Tyr[550] probably does not play a significant role in tyrosine phosphorylation of the receptor because this protein was still tyrosine phosphorylated on immunoblots, and agonist-evoked current run-down, which could be prevented by tyrosine phosphatase inhibitors, was still observed. In contrast, little or no tyrosine phosphorylation of P2X$_7$[Y343F] protein was detected; in this mutant, currents showed only P2X$_2$ receptor-like run-down and this was not affected by tyrosine phosphatase inhibitors. The phosphatase inhibitors also did not alter the time to initial membrane blebbing in the P2X$_7$[Y343F] receptor. Such results provide fairly conclusive evidence that Tyr[343] is the major residue that is dephosphorylated by receptor activation.

The involvement of Tyr[343] in the action of the phosphatase inhibitors was at first surprising because it had previously been thought to be situated well within the second transmembrane domain of the receptor. Tyrosine at this position is found only in the P2X$_7$ receptor; the other subunits have isoleucine, leucine, serine or tryptophan. One must consider the possibility that Tyr[343] is not directly phosphorylated and that the mutation Y343F (and Y343C) results in a conformational change of the protein such that the run-down of the current is prevented. This seems very unlikely because mutations of no other tyrosine prevented the action of the phosphatase inhibitors. Therefore, Tyr[343] should itself be accessible to kinase and phosphatase. Hydrophobicity plots indicate that a segment of ~26 amino acids (Phe[328]–Ile[355]) is likely to contribute to the second transmembrane of the P2X$_7$ receptor. Secondary structure prediction algorithms indicate that this is likely to be helical and that the first two-thirds of it would be strongly amphipathic. One face would be exposed to lipid and one side, containing Tyr[343], exposed to protein or water. Figure 6B depicts schematically how this might result in accessibility of Tyr[343] to phosphorylation.

In the case of the NMDA receptor subunits NR1 and NR2, tyrosine residues were identified as playing a role in run-down of the membrane current with repeated applications (Vissel *et al*., 2001). In that case also, the run-down was not observed with NMDA subunits in which critical tyrosine residues had been substituted by phenylalanine residues. The tyrosines were also located at the interface between the final transmembrane domain and the

beginning of the C-terminal tail, and the run-down of the current resulted from association with an adaptor protein (Vissel *et al.*, 2001). It seems possible that a similar interaction between this part of the P2X$_7$ receptor and an associated protein could underlie the similar functional picture. Phosphorylation at Tyr^{343} might be necessary for the interaction of another protein with the P2X$_7$ receptor because Y343F mutation also showed an impaired ability to couple to cytoskeletal elements and bring about blebbing formation.

Significance of P2X$_7$ receptor signalling complex

There are now several cases known of interactions between membrane ion channels and specific cytoskeletal elements (Sheng and Pak, 2000). In those cases, the emphasis has been largely on 'inside-out' signalling. That is to say, the results have been interpreted in terms of the associated proteins and the cytoskeleton altering the distribution and function of the channels. The P2X$_7$ receptor is unique because it has been well characterized as initiating 'outside-in' signalling (see Introduction). Activation of the P2X$_7$ receptor itself rapidly engages the cytoskeleton and brings about changes in cell shape and form. The present experiments have identified some of the initial molecular steps in this process and they have also shown how it might be controlled through feedback alterations in receptor phosphorylation of an identified tyrosine located at the inner membrane interface. They provide a framework for the further analysis of the increasing distinction between the flow of ionic current and direct protein–protein interactions in the cell physiology of P2X$_7$ receptors.

Materials and methods

Purification of P2X$_7$ receptor complex by immunoprecipitation

The receptor complex was isolated from HEK293 cells stably expressing rat P2X$_7$ receptor using immunoprecipitation with ecto-P2X$_7$ Ab (Kim *et al.*, 2001). In brief, the receptor complex was incubated with solubilization buffer [20 mM dodecylmaltoside (DM) in phosphate-buffered saline (PBS) containing protease inhibitors] from purified membrane fractions, followed by pre-absorption of background proteins with γ-bind G-Sepharose, incubation with ecto-P2X$_7$ Ab and subsequent γ-bind G-Sepharose precipitation. After overnight incubation at 4°C, the resins were washed with 10 vols of solubilization buffer and proteins were separated from the resin by boiling for 5 min in SDS sample buffer.

In-gel digestion and MALDI-TOF MS

The in-gel digestion of the proteins was performed with some modifications according to Shevchenko *et al.* (1996). Receptor complex samples were separated by SDS–PAGE. The Coomassie-stained gel pieces were decoloured by repeated cycles of dehydration with 50% acetonitrile (ACN) in 50 mM NH$_4$HCO$_3$ pH 8.4 and hydration with 50 mM NH$_4$HCO$_3$. The destained protein bands were shrunk by dehydration in ACN and dried in a vacuum centrifuge. The protein bands were reduced with 10 mM dithiothreitol (DTT) in 100 mM NH$_4$HCO$_3$ for 1 h at 56°C. For alkylation of proteins, the DTT solution was replaced by 55 mM iodoacetic acid in 100 mM NH$_4$HCO$_3$ and incubated for 1 h in the dark. The reduced, alkylated gel pieces were washed with 100 mM NH$_4$HCO$_3$, dehydrated with ACN, swollen in 100 mM NH$_4$HCO$_3$, and shrunk again by ACN. The liquid phase was removed, and the gel pieces were completely dried in a vacuum centrifuge. The gel pieces were incubated overnight at 37°C with endoprotease Asp-N (50 mM sodium phosphate buffer pH 8.0), endoprotease Arg-C (100 mM Tris–HCl pH 7.6, 10 mM CaCl$_2$, 5 mM DTT, 0.5 mM EDTA) or trypsin (50 mM Tris–HCl pH 7.6, 1 mM CaCl$_2$). Protease-digested supernatants were adjusted to 0.1% trifluoroacetic acid (TFA) by addition of 10% TFA. The peptide fragments were desalted, concentrated with ZipTip$_{C18}$ and finally eluted with matrix solution

(α-cyano-cinnamic acid in 50% ACN/0.1% TFA). Samples were prepared using dried-drop method, by dropping sample-matrix solution directly onto target plate. Mass spectra were obtained using a TofSpecE MALDI-TOF mass spectrometer (Micromass, Manchester, UK) equipped with a reflectron mode for increased mass accuracy in positive ion. Mass spectra were either externally calibrated or mass converted using internal calibrants with MassLynx program. Proteins were identified based on matching the MS data with mass values of calculated peptide fragments using ProFound (prowl.rockefeller.edu), PeptIdent (www.expasy.ch) and Peptide Mass (www.expasy.ch).

Immunoblot analysis

Immunoprecipitated P2X$_7$ complex proteins were separated by SDS–PAGE and western blots were performed as described previously (Kim *et al.*, 2001). For detection of tyrosine-phosphorylated proteins, the following modifications were used. Cells were lysed immediately, solubilized with solubilization buffer containing 20 mM DM, 500 μM bpV and protease inhibitors (Complete™ EDTA-free) in PBS for 1 h at 4°C, followed by immunoprecipitation with either ecto-P2X$_7$ Ab, anti-EE Ab or mouse IgG as control. Membranes were immunoblotted with either anti-phosphotyrosine Ab PY20 or polyclonal anti-P2X$_7$ receptor Ab. For western blotting of anti-phosphotyrosine Ab, blocking buffer [1% bovine serum albumin (BSA), 10 mM Tris pH 7.5, 100 mM NaCl, 0.1% Tween 20] was used. To examine protein–protein interaction between PI4K230 (HA-tagged) and P2X$_7$ receptor, co-transfection of these cDNAs was performed, after which immunoprecipitation with anti-EE or anti-HA Ab and blot with anti-HA Ab or C-terminal polyclonal P2X$_7$ Ab was carried out. When appropriate, the membranes were stripped with Restore™ western blot stripping buffer and reprobed with a different antibody. Protein bands on films were semi-quantitatively analysed by densito-metric scanning via GeneSnap and GeneTools software (Syngene, Cambridge, UK). All experiments were repeated 3–10 times with similar results obtained throughout.

Mutagenesis and electrophysiology

Mutations were introduced into the rat P2X$_7$ cDNA with a Glu-Glu (GLNEYMPME) tag at its C-terminus (P2X$_7$-EE) in pcDNA3.1+, by the 'quick change mutagenesis' method using Pfu Turbo® polymerase (Stratagene). Sequences were verified for the entire open reading frame, by ABI Big Dye® sequencing (PE Biosystems). Standard whole-cell recordings and measurements of time to membrane blebbing were performed as described previously (Virginio *et al.*, 1999). BzATP (100 μM) was typically applied for 4 s, at 2 min intervals. Inhibition by bpV was quantitated by measuring the amplitude of the current evoked by the sixth application of BzATP as a fraction of the amplitude of the current evoked by the first application (x); this was done in the presence of bpV ($x \approx 1$) and after washout of bpV ($x' < 1$). The fraction x'/x was normalized to the change in current observed with a maximal concentration of bpV (100 μM) and the results fit with a logistic function. All data are shown as mean ± SEM and tests for significance were by Mann–Whitney non-parametric analysis.

Chemicals and antibodies

DM, bpV, mpV and 3,4-dephostatin were purchased from Calbiochem (San Diego, CA), Complete™, endoprotease Asp-N, endoprotease Arg-C and trypsin (sequencing grade) were from Roche (Indianapolis, IN), ZipTip$_{C18}$ from Millipore (Bedford, MA), γ-bind G-Sepharose from Amersham Pharmacia (Uppsala, Sweden), Restore™ western blot stripping buffer from Pierce (Rockford, IL). All other chemicals were from Sigma. Anti-RPTPβ, anti-Hsp90 and anti-phosphotyrosine (PY20) antibodies were from Transduction Laboratories (San Diego, CA), anti-β-actin and anti-α-actinin from Sigma, anti-Hsp70 from Calbiochem, anti-Hsc70 from Alexis Biochemicals (San Diego, CA), anti-integrin β2 from Oncogene Research Products (Cambridge, MA), anti-EE and anti-HA from BabCo (Berkeley, CA), C-terminal anti-P2X$_7$ and C-terminal anti-P2X$_2$ (polyclonals) from Alomone (Jerusalem, Israel), and ecto-P2X$_7$ (monoclonal) as described previously (Kim *et al.*, 2001). Anti-p55 MAGuK Ab (Ruff *et al.*, 1991) was supplied by Dr A.Chishti (Tufts University), anti-laminin α3 (Hirosaki *et al.*, 2000) by Dr K.Miyazaki (Yokohama City University), anti-supervillin (Pestonjamasp *et al.*, 1997) by Dr E.Luna (University of Massachusetts, Worcester) and HA-tagged PI4K230 cDNA (Gehrmann *et al.*, 1999) by Professor L.Heilmeyer (Ruhr-Universitat Bochum).

Acknowledgements

References

Bohnsack,J.F., Akiyama,S.K., Damsky,C.H., Knape,W.A. and Zimmerman, G.A. (1990) Human neutrophil adherence to laminin *in vitro*. Evidence for a distinct neutrophil integrin receptor for laminin. *J. Exp. Med.*, **171**, 1221–1237.

Bronte,V., Macino,B., Zambon,A., Rosato,A., Mandruzzato,S., Zanovello,P. and Collavo,D. (1996) Protein tyrosine kinase inhibitors and phosphatases control apoptosis induced by extracellular adenosine 5′-triphosphate. *Biochem. Biophys. Res. Commun.*, **218**, 344–351.

Caplan,A.J. (1999) Hsp90's secrets unfold: new insights from structural and functional studies. *Trends Cell Biol.*, **9**, 262–268.

Cohn,Z.A. and Parks,E. (1967) The regulation of pinocytosis in mouse macrophages. III. The induction of vesicle formation by nucleosides and nucleotides. *J. Exp. Med.*, **125**, 457–466.

Collo,G., Neidhart,S., Kawashima,E., Kosco-Vilbois,M., North,R.A. and Buell,G. (1997) Tissue distribution of the P2X$_7$ receptor. *Neuropharmacology*, **36**, 1277–1283.

Colognato,H. and Yurchenco,P.D. (2000) Form and function: the laminin family of heterotrimers. *Dev. Dyn.*, **218**, 213–234.

Dimitratos,S.D., Woods,D.F., Stathakis,D.G. and Bryant,P.J. (1999) Signaling pathways are focused at specialized regions of the plasma membrane by scaffolding proteins of the MAGuK family. *BioEssays*, **21**, 912–921.

Di Virgilio,F. (2000) Dr Jekyll/Mr Hyde: the dual role of extracellular ATP. *J. Auton. Nerv. Syst.*, **81**, 59–63.

Ferrari,D., Chiozzi,P., Falzoni,S., Dal Susino,M., Melchiorri,L., Baricordi,O.R. and Di Virgilio,F. (1997a) Extracellular ATP triggers IL-1β release by activating the purinergic P2Z receptor of human macrophages. *J. Immunol.*, **159**, 1451–1458.

Ferrari,D., Wesselborg,S., Bauer,M.K. and Schulze-Osthoff,K. (1997b) Extracellular ATP activates transcription factor NF-κB through the P2Z purinoreceptor by selectively targeting NF-κB p65. *J. Cell Biol.*, **139**, 1635–1643.

Fischer,E.H., Charbonneau,H. and Tonks,N. (1991) Protein tyrosine phosphatases: a diverse family of intracellular and transmembrane proteins. *Science*, **253**, 401–406.

Gehrmann,T. and Heilmeyer,L.M.,Jr (1998) Phosphatidylinositol 4-kinases. *Eur. J. Biochem.*, **253**, 357–370.

Gehrmann,T., Gulkan,H., Suer,S., Herberg,F.W., Balla,A., Vereb,G., Mayr,G.W. and Heilmeyer,L.M.,Jr (1999) Functional expression and characterization of a new human phosphatidylinositol 4-kinase PI4K230. *Biochim. Biophys. Acta*, **1437**, 341–356.

Gudipaty,L., Humphreys,B.D., Buell,G. and Dubyak,G.R. (2001) Regulation of P2X$_7$ nucleotide receptor function in human monocytes by extracellular ions and receptor density. *Am. J. Physiol.*, **280**, C943–C953.

Hibell,A.D., Kidd,E.J., Chessell,I.P., Humphrey,P.P. and Michel,A.D. (2000) Apparent species differences in the kinetic properties of P2X$_7$ receptors. *Br. J. Pharmacol.*, **130**, 167–173.

Hirosaki,T., Mizushima,H., Tsubota,Y., Moriyama,K. and Miyazaki,K. (2000) Structural requirement of carboxyl-terminal globular domains of laminin α3 chain for promotion of rapid cell adhesion and migration of laminin 5. *J. Biol. Chem.*, **275**, 22495–22502.

Holmes,T.C., Fadool,D.A. and Levitan,I.B. (1996) Tyrosine phosphorylation of the Kv1.3 potassium channel. *J. Neurosci.*, **16**, 1581–1590.

Humphreys,B.D. and Dubyak,G.R. (1996) Induction of the P2z/P2X7 nucleotide receptor and associated phospholipase D activity by lipopolysaccharide and IFN-γ in the human THP-1 monocytic cell line. *J. Immunol.*, **157**, 5627–5637.

Husi,H., Ward,M.A., Choudhary,J.S., Blackstock,W.P. and Grant,S.G. (2000) Proteomic analysis of NMDA receptor–adhesion protein signaling complexes. *Nature Neurosci.*, **3**, 661–669.

Kellerer,M., Mushack,J., Mischak,H. and Haring,H.U. (1997) Protein kinase C (PKC) ε enhances the inhibitory effect of TNFα on insulin signaling in HEK293 cells. *FEBS Lett.*, **418**, 119–122.

Kim,M., Spelta,V., Sim,J., North,R.A. and Surprenant,A. (2001)

Differential assembly of rat purinergic P2X$_7$ receptor in immune cells of the brain and periphery. *J. Biol. Chem.*, **276**, 23262–23267.

Koyasu,S., Nishida,E., Kadowaki,T., Matsuzaki,F., Iida,K., Kasuga,M., Sakai,H. and Yahara,I. (1986) Two mammalian heat shock proteins, Hsp90 and Hsc100, are actin binding proteins. *Proc. Natl Acad. Sci. USA*, **83**, 8054–8058.

Krupp,J.J., Vissel,B., Thomas,C.G., Heinemann,S.F. and Westbrook, G.L. (1999) Interactions of calmodulin and α-actinin with the NR1 subunit modulate Ca^{2+}-dependent inactivation of NMDA receptors. *J. Neurosci.*, **19**, 1165–1178.

Ling,S., Woronuk,G., Lev,S. and Braun,A.P. (2000) Enhanced activity of a large conductance calcium-sensitive K channels in the presence of Src tyrosine kinase. *J. Biol. Chem.*, **275**, 30683–30689.

Michel,A.D., Chessell,I.P. and Humphrey,P.P. (1999) Ionic effects on human recombinant P2X$_7$ receptor function. *Naunyn Schmiedebergs Arch. Pharmakol.*, **359**, 102–109.

Moss,S.J., Gorrie,G.H., Amato,A. and Smart,T.G. (1995) Modulation of GABA-A receptors by tyrosine phosphorylation. *Nature*, **377**, 344–348.

Mutini,C., Falzoni,S., Ferrari,D., Chiozzi,P., Morelli,A., Baricordi,O.R., Collo,G., Ricciardi-Castagnoli,P. and Di Virgilio,F. (1999) Mouse dendritic cells express the P2X$_7$ purinergic receptor: characterization and possible participation in antigen presentation. *J. Immunol.*, **163**, 1958–1965.

Nicke,A., Baumert,H.G., Rettinger,J., Eichele,A., Lambrecht,G., Mutschler,E. and Schmalzing,G. (1998) P2X$_1$ and P2X$_3$ receptors form stable trimers: a novel structural motif of ligand-gated ion channels. *EMBO J.*, **17**, 3016–3028.

North,R.A. and Surprenant,A. (2000) Pharmacology of cloned P2X receptors. *Annu. Rev. Pharmacol. Toxicol.*, **40**, 563–580.

Pestonjamasp,K.N., Pope,R.K., Wulfkuhle,J.D. and Luna,E.J. (1997) Supervillin (p205): a novel membrane-associated, F-actin-binding protein in the villin/gelsolin superfamily. *J. Cell Biol.*, **139**, 1255–1269.

Posner,B.I. *et al.* (1994) Peroxovanadium compounds. A new class of potent phosphotyrosine inhibitors which are insulin mimetics. *J. Biol. Chem.*, **269**, 4596–4604.

Rassendren,F., Buell,G.N., Virginio,C., Collo,G., North,R.A. and Surprenant,A. (1997) The permeabilizing ATP receptor, P2X$_7$. Cloning and expression of a human cDNA. *J. Biol. Chem.*, **272**, 5482–5486.

Ratcliffe,C.E., Qu,Y., McCormick,K.A., Tibbs,V.C., Dixon,J.E., Scheuer,T. and Catterall,W.A. (2000) A sodium channels signalling complex: modulation by associated receptor tyrosine phosphatase β. *Nature Neurosci.*, **3**, 437–444.

Rosenmund,C. and Westbrook,G. (1993) Calcium-induced actin depolymerization reduces NMDA channel activity. *Neuron*, **10**, 805–814.

Ruff,P., Speicher,D.W. and Chishti,A. (1991) Molecular identification of a major palmitoylated erythrocyte membrane protein containing the src homology 3 motif. *Proc. Natl Acad. Sci. USA*, **88**, 6595–6599.

Sampath,R., Gallagher,P.J. and Pavalko,F.M. (1998) Cytoskeletal interactions with the leukocyte integrin β2 cytoplasmic tail. Activation-dependent regulation of associations with talin and α-actinin. *J. Biol. Chem.*, **273**, 33588–33594.

Sheng,M. and Pak,D.T. (2000) Ligand-gated ion channel interactions with cytoskeletal and signaling proteins. *Annu. Rev. Physiol.*, **62**, 755–778.

Shevchenko,A., Wilm,M., Vorm,O. and Mann,M. (1996) Mass spectrometric sequencing of proteins from silver-stained poly-acrylamide gels. *Anal. Chem.*, **66**, 850–858.

Solle,M., Labasi,J., Perregaux,D.G., Stam,E., Petrushova,N., Koller, B.H., Griffiths,R.J. and Gabel,C.A. (2001) Altered cytokine production in mice lacking P2X(7) receptors. *J. Biol. Chem.*, **276**, 125–132.

Surprenant,A., Rassendren,F., Kawashima,E., North,R.A. and Buell,G. (1996) The cytolytic P2Z receptor for extracellular ATP identified as a P2X receptor (P2X7). *Science*, **272**, 735–738.

Torres,G.E., Egan,T.M. and Voigt,M.M. (1999) Hetero-oligomeric assembly of P2X receptor subunits. Specificities exist with regard to possible partners. *J. Biol. Chem.*, **274**, 6653–6659.

Virginio,C., MacKenzie,A., North,R.A. and Surprenant,A. (1999) Kinetics of cell lysis, dye uptake and permeability changes in cells expressing the rat P2X$_7$ receptor. *J. Physiol.*, **519**, 335–346.

Vissel,B., Krupp,J.J., Heinemann,S.F. and Westbrook,G.L. (2001) A use-dependent tyrosine dephosphorylation of NMDA receptors is independent of ion flux. *Nature Neurosci.*, **4**, 587–596.

Wulfkuhle,J.D., Donina,I.E., Stark,N.H., Pope,R.K., Pestonjamasp,K.N., Niswonger,M.L. and Luna,E.J. (1999) Domain analysis of supervillin, an F-actin bundling plasma membrane protein with functional nuclear localization signals. *J. Cell Sci.*, **112**, 2125–2136.

Yang,M. and Leonard,J.P. (2001) Identification of mouse NMDA receptor subunit NR2A C-terminal tyrosine sites phosphorylated by co-expression with v-Src. *J. Neurochem.*, **77**, 580–588.

Yu,X.-M., Askalan,R., Keil,G.J. and Salter,M.W. (1997) NMDA channel regulation by channel-associated protein tyrosine kinase Src. *Science*, **275**, 674–678.

Zheng,F., Gingrich,M.B., Traynelis,S.F. and Conn,P.J. (1998) Tyrosine kinase potentiates NMDA receptor currents by reducing tonic zinc inhibition. *Nature Neurosci.*, **1**, 185–191.